Hubble Space Telescope

Cycle 15 GO Proposal

Decelerating and Dustfree: Efficient Dark Energy Studies with Supernovae and Clusters

Principal Investigator: Prof. Saul Perlmutter

Institution: University of California - Berkeley

Electronic Mail: saul@lbl.gov

Scientific Category: COSMOLOGY

Scientific Keywords: COSMOLOGICAL PARAMETERS AND DISTANCE SCALE, CLUSTERS OF GALAXIES, SUPERNOVAE

Instruments: ACS, NICMOS

Proprietary Period: 12

Orbit Request	Prime	Parallel
Cycle 15	217	34

Abstract

Our cycle 14 program has proved a new, extremely efficient approach to obtain z>1 dust-free Type Ia supernovae, and we propose to capitalize on this new technique. We will collect a total sample of ~20 z>1 SNe Ia in cluster elliptical galaxies, each of which will carry the weight of up to 9 color-corrected z>1 SNe hosted by spiral galaxies. The measurement will yield dark energy constraints that do not suffer from the major systematic and statistical uncertainty at these redshifts, that of extinction correction. By targeting massive galaxy clusters at z>1, we probe a well-understood host galaxy environment, and obtain more than five-times higher efficiency than a survey of random fields in detection of Ia supernovae in elliptical galaxies. The data will make possible a factor of two improvement on supernova constraints on dark energy time evolution dynamics, and a much larger improvement on systematic uncertainty, taking advantage of the uniquely well-controlled host environment that clusters provide. These same deep cluster images also yield fundamental mass calibrations required for ongoing and future studies which aim to measure dark energy via the evolution of cluster abundances, as well as an entire program of cluster studies. We will obtain both a cluster dataset and a SN Ia dataset that will be a longstanding scientific resource.

Investigators:

	Investigator	Institution	Country
PI	Prof. Saul Perlmutter	University of California - Berkeley	USA/CA
CoI	Dr. Greg Aldering	Lawrence Berkeley National Laboratory	USA/CA
CoI	Mr. Rahman Amanullah	Stockholm University	Sweden
CoI	Mr. Kyle Barbary	University of California - Berkeley	USA/CA
CoI	Prof. L Felipe Barrientos	Universidad Catolica de Chile	Chile
CoI	Dr. Mark Brodwin	Jet Propulsion Laboratory	USA/CA
CoI	Dr. Kyle Dawson	Lawrence Berkeley National Laboratory	USA/CA
CoI	Dr. Arjun Dey	National Optical Astronomy Observatory	
CoI	Dr. Mamoru Doi	University of Tokyo, Institute of Astronomy	Japan
CoI	Dr. Megan Donahue	Michigan State University	USA/MI
CoI	Dr. Peter Eisenhardt	Jet Propulsion Laboratory	USA/CA
CoI	Dr. Erica Ellingson	University of Colorado at Boulder	USA/CO
CoI	Dr. Vitaliy Fadeyev	Lawrence Berkeley National Laboratory	USA/CA
CoI	Dr. Andrew Fruchter	Space Telescope Science Institute	USA/MD
CoI	Dr. David Gilbank	University of Toronto	Canada
CoI	Dr. Michael Gladders	Carnegie Institution of Washington	USA/DC
CoI	Dr. Gerson Goldhaber	Lawrence Berkeley National Laboratory	USA/CA
CoI	Dr. Anthony H. Gonzalez	University of Florida	USA/FL
CoI*	Dr. Ariel Goobar	Stockholm University	Sweden
CoI	Dr. Joseph Hennawi	University of California - Berkeley	USA/CA
CoI	Dr. Henk Hoekstra	University of Victoria	Canada
CoI*	Dr. Isobel Hook	University of Oxford	UK
CoI	Dr. Buell T. Jannuzi	National Optical Astronomy Observatories, AURA	USA/AZ
CoI	Dr. David Johnston	Jet Propulsion Laboratory	USA/CA
CoI	Dr. Nobunari Kashikawa	National Astronomical Observatory of Japan (NAOJ)	Japan
CoI	Dr. Marek Kowalski	Lawrence Berkeley National Laboratory	USA/CA
CoI	Dr. Natalia Kuznetsova	Lawrence Berkeley National Laboratory	USA/CA
CoI	Dr. Wonyong Lee	Lawrence Berkeley National Laboratory	USA/CA
CoI*	Dr. Christopher Lidman	European Southern Observatory - Chile	Chile
CoI	Dr. Eric Linder	University of California - Berkeley	USA/CA
CoI	Prof. Lori M. Lubin	University of California - Davis	USA/CA

	Investigator	Institution	Country
CoI	Mr. Tomoki Morokuma	University of Tokyo, Institute of Astronomy	Japan
CoI	Dr. Chris Mullis	University of Michigan	USA/MI
CoI	Dr. Nino Panagia	Space Telescope Science Institute	USA/MD
CoI	Dr. Marc Postman	Space Telescope Science Institute	USA/MD
CoI	Dr. Jason Rhodes	Jet Propulsion Laboratory	USA/CA
CoI*	Dr. Piero Rosati	European Southern Observatory - Germany	Germany
CoI	Mr. David Rubin	University of California - Berkeley	USA/CA
CoI	Dr. David J. Schlegel	Lawrence Berkeley National Laboratory	USA/CA
CoI	Dr. Anthony L. Spadafora	Lawrence Berkeley National Laboratory	USA/CA
CoI	Dr. S. Adam Stanford	University of California - Davis	USA/CA
CoI*	Dr. Vallery Stanishev	Stockholm University	Sweden
CoI	Dr. Daniel Stern	Jet Propulsion Laboratory	USA/CA
CoI	Dr. Nao Suzuki	Lawrence Berkeley National Laboratory	USA/CA
CoI	Dr. Lifan Wang	Lawrence Berkeley National Laboratory	USA/CA
CoI	Dr. Naoki Yasuda	University of Tokyo, Institute of Cosmic Ray Research	Japan
CoI	Dr. Howard K. Yee	University of Toronto	Canada

Number of investigators: 47

* ESA investigators: 5

Target Summary:

Target	RA	Dec	Magnitude
WARPS1415+36	14 15 11.1000	+36 12 3.00	V = 25.0
1012.28	14 34 28.5200	+34 26 22.90	V = 25.0
1012.52	14 32 29.1800	+33 32 48.30	V = 25.0
1113.7.7	14 29 18.5100	+34 37 25.80	V = 25.0
1214.5.28	14 32 38.2800	+34 36 49.00	V = 25.0
1315.5.16	14 38 9.5400	+34 14 19.20	V = 25.0
1315.12	14 34 46.3300	+35 19 45.80	V = 25.0
1416.7.15	14 33 51.1300	+33 25 51.10	V = 25.0
IRAC0223-04	02 23 3.7000	-04 36 18.00	V = 25.0
RCS0220-03	02 20 55.7000	-03 33 19.00	V = 25.0
RCS0221-03	02 21 41.9500	-03 21 47.40	V = 25.0

Target	RA	Dec	Magnitude
RCS0337-28	03 37 50.4000	-28 44 28.70	V = 25.0
RCS0439-29	04 39 38.0400	-29 04 55.20	V = 25.0
RCS1511+09	15 11 3.8000	+09 03 15.00	V = 25.0
RCS2156-04	21 56 42.1500	-04 48 4.10	V = 25.0
RCS2319+00	23 19 53.3800	+00 38 13.90	V = 25.0
RCS2345-36	23 45 27.3000	-36 32 50.00	V = 25.0
RDCS0848+44	08 48 58.6400	+44 51 57.00	V = 25.0
RDCS1252-29	12 52 54.2800	-29 27 17.90	V = 25.0
XMM3	21 45 0.0000	+01 15 0.00	V = 25.0
XMMUJ2235	22 35 20.8300	-25 57 39.90	V = 25.0
XMMUJ1229+01	12 29 28.8000	+01 51 34.00	V = 25.0
CL1604+43	16 04 22.6000	+43 04 39.70	V = 25.0
TOO-SN-11ORB	14 16 30.0000	+32 30 0.00	V = 25.0
TOO-SN-2ORB	08 48 0.0000	+44 00 0.00	V = 25.0
TOO-SN-1ORB	12 52 0.0000	-29 00 0.00	V = 25.0

Observing Summary:

Target	Config Mode and Spectral Elements	Flags	Orbits
WARPS1415+36	ACS/WFC Imaging F850LP		9 (1x9)
1012.28	ACS/WFC Imaging F850LP		9 (1x9)
1012.52	ACS/WFC Imaging F850LP		9 (1x9)
1113.7.7	ACS/WFC Imaging F850LP		9 (1x9)
1214.5.28	ACS/WFC Imaging F850LP		9 (1x9)
1315.5.16	ACS/WFC Imaging F850LP		10 (1x10)
1315.12	ACS/WFC Imaging F850LP		10 (1x10)
1416.7.15	ACS/WFC Imaging F850LP		10 (1x10)
IRAC0223-04	ACS/WFC Imaging F850LP		6 (1x6)
RCS0220-03	ACS/WFC Imaging F850LP		6 (1x6)
RCS0221-03	ACS/WFC Imaging F850LP		6 (1x6)

Prof. Saul Perlmutter

Decelerating and Dustfree: Efficient Dark Energy Studies with Supernovae and Clusters

Target	Config Mode and Spectral Elements	Flags	Orbits
RCS0337-28	ACS/WFC Imaging F850LP		8 (1x8)
RCS0439-29	ACS/WFC Imaging F850LP		8 (1x8)
RCS1511+09	ACS/WFC Imaging F850LP		8 (1x8)
RCS2156-04	ACS/WFC Imaging F850LP		6 (1x6)
RCS2319+00	ACS/WFC Imaging F850LP		6 (1x6)
RCS2345-36	ACS/WFC Imaging F850LP		8 (1x8)
RDCS0848+44	ACS/WFC Imaging F850LP		7 (1x7)
RDCS1252-29	ACS/WFC Imaging F850LP		7 (1x7)
XMM3	ACS/WFC Imaging F850LP		8 (1x8)
XMMUJ2235	ACS/WFC Imaging F850LP		8 (1x8)
XMMUJ1229+01	ACS/WFC Imaging F850LP		7 (1x7)
CL1604+43	ACS/WFC Imaging F850LP		9 (1x9)
TOO-SN-11ORB	NIC2 Imaging F110W	TOO	22 (11x2)
TOO-SN-2ORB	NIC2 Imaging F110W	TOO	4 (2x2)
TOO-SN-1ORB	NIC2 Imaging F110W	TOO	8 (1x8)

Total prime orbits: 217

Scientific Justification

Using Type Ia Supernovae in Early-type Galaxies to Measure Cosmology

The signature goal of the most ambitious cosmology projects being designed or built this decade (LSST/LST/Panstarrs, Dark Energy Camera, JDEM/SNAP/Destiny, the South Pole Telescope and other SZ experiments) is the detailed, accurate measurement of the universe's expansion history, from deceleration through acceleration, to look for clues of the properties and identity of dark energy. Of the known measurement techniques (SNe Ia, cluster counts, S-Z, weak lensing, and baryon oscillations), only Type Ia supernovae (SNe Ia) have actually been developed to the point of routine use. Only HST observations can provide the required signal-to-noise for those SNe at $z \gtrsim 1$, where the transition from deceleration to acceleration can be studied. Initial studies of the decelerating universe from both the Higher-Z Team (Riess *et al.* 2004) and the Supernova Cosmology Project (Fadeyev, Aldering *et al.* 2004) clearly point to the limiting factor for both statistical and systematic uncertainties: host-galaxy-extinction correction.

In Cycle 14, we are successfully demonstrating a new, highly efficient approach to the measurements in this difficult decelerating redshift range. By discovering and studying "clean" SNe in galaxy cluster ellipticals we dramatically reduce systematic and statistical uncertainties (each of these SNe is worth up to *nine* SNe in spirals) — and do so with a dramatically more efficient use of HST time. So far we have obtained lightcurves of 5 $z > 1$ SNe using 81 orbits, which is more than twice the rate of previous GOODS surveys (see below). Here we propose to reap the full benefits from this approach.

Using the Cycle 14 sample of high-redshift clusters allows us not only to start the Cycle 15 SN search with extremely deep reference images, but also to add a second filter, F775W, to the F850LP data, enabling a major step forward in the cluster science and other comsological measurement techniques. In particular, counting clusters is an extremely sensitive measure of expansion history, if their masses can be estimated with reasonable precision. With the addition of deep F775W data, we propose to study cluster masses via weak lensing from the same HST images, and calibrate Sunyaev-Zeldovich/X-Ray distance measurements to those same clusters. We have intentionally included clusters that are X-ray-selected, optically-selected, and IR-selected for this purpose. Finally, this data set will be used to study massive galaxy assembly and star formation rates by measuring the intrinsic scatter of the red sequence.

How problematic is the extinction correction uncertainty at $z \gtrsim 1$? The correction for extinction from dust in the host galaxies is currently the single dominant source of both statistical and systematic error for SNe distances and the derived cosmological parameters – dramatically so at $z > 1$ even with HST (see Figure 1b). The typical color uncertainty for HST-studied $z > 1$ SNe is 0.06 – 0.1 in $B - V$, leading to uncertainties in extinction correction (after accounting for intrinsic color uncertainty) of as high as ∼0.4 mag! This dispersion grows worse, $\sigma \approx 0.5$, after accounting for the uncertainty in the dust reddening coefficient, $R_B \equiv A_B/E(B-V)$, which Draine (2003) notes can vary from the fiducial value 4.1 by ± 0.5 and for which empirical studies of multiband SNe colors indicate an even wider range. (The actual dispersion about the Hubble-line fit for $z > 1$ SNe Ia fully corrected for extinction matches this 0.5 mag value.) Figure 2a shows the resulting poor constraints on the dark-energy equation-of-state parameter and its time variation, w_0 vs. w'.

These constraints are insufficient to distinguish between almost any current dark energy model.

To correct for dust extinction, either one needs exquisitely good multi-band color information, or one is driven to use a Bayesian prior on $a)$ the mean and probability distribution of R_B and $b)$ the probability distribution of the amount of dust. If even just one of these priors is redshift dependent, the final result will be systematically biased. The effect of varying R_B can be seen in Fig. 2b as the difference between full and the short-dashed contour. Likewise, if the observation quality depends on redshift (as is often the case) significant biases can result, as shown by the difference between the full and the long-dashed contour of Fig. 2b (Perlmutter *et al.* 1999). If aggressive Bayesian priors are chosen, the larger systematic errors outweigh the smaller statistical errors.

How is this problem solved using SNe Ia in cluster ellipticals? In Sullivan *et al.* (2003), we showed that the dispersion (including ground-based measurement error) about the Hubble diagram for elliptical-hosted SNe is 0.16 mag — nearly three times smaller than just the measurement uncertainty for extinction-corrected SNe Ia at $z > 1$ — primarily due to the absence of dust. (Preliminary studies of the new, larger SNe sample from the CFHT SNe Legacy Survey indicate the same thing.) Thus, each elliptical SNe Ia is statistically worth up to $\sim$9 SNe Ia in spirals when making cosmological measurements – and without the aforementioned systematics associated with extinction correction.

At redshifts $z \gtrsim 1$ only elliptical galaxies in clusters are sufficiently quiescent to be dust free, while elliptical field galaxies may still host a non-negligible amount of dust. We therefore propose to complete a sample of $\sim$20 SNe Ia ($\sim$10 each in Cycles 14 and 15) at $z \gtrsim 1$ entirely in cluster elliptical host galaxies, to achieve the statistical constraints of $\sim$150 SNe in later-type hosts. (This sample's statistical strength is almost enough to match the large, well-measured CFHT Legacy Survey samples of elliptical hosted SNe at $z \lesssim 0.8$, to obtain "dust-free Hubble diagrams.") This cluster-ellipticals-only sample will yield the stronger constraints on w vs. w' shown in Fig. 2c — without extinction prior systematics. In particular, this would provide a test of the small, suggestive shift from a cosmological constant model seen in Riess et al 2004 (Fig. 2b shaded contour). Next in priority are SNe found in elliptical field galaxies, and then SNe in spiral galaxies, which will be found and studied without extra costs. The $z = 0.9 - 1.6$ redshift range provides key leverage of the cosmological model, especially constraints on the dark energy time variation w'.

How is it known that dust is not an issue in $z \gtrsim 1$ cluster ellipticals? Although evidence for dust is found in $\sim 50\%$ of nearby ellipticals, the quantity of dust is generally very small and confined to the central few hundred pc (e.g. Tran *et al.* 2001). Recent Spitzer data (Temi *et al.* 2005) confirms that most nearby ellipticals have the SED's expected for dust-free systems. While field ellipticals at larger redshifts do show signs of increasing star-formation in that blue clumps have been detected in nearly 50 % of them at $z \sim 1$ (Pasquali *et al.* 2006), blue clumps are *not* found in cluster ellipticals at $z \sim 1$. The clearest evidence that dust has little effect on stars in cluster elliptical galaxies comes from the tightness of their color-magnitude relations. The dispersion in the colors of early-type galaxies is very small in clusters ranging from Coma to intermediate redshifts (Bower *et al.* 1992; Ellis *et al.* 1997; Stanford, Eisenhardt & Dickinson 1998; van Dokkum *et al.* 2001). In fact, this relation has been shown by Hogg *et al.* (2004) to be universal for early-type galaxies in clusters and in lower-density environments using an enormous sample from SDSS.

Results from ACS imaging show the same strikingly small dispersion in color extends to

redshifts $z \gtrsim 1$ (Figure 3). ACS imaging of RDCS1252-29 at $z = 1.23$ by Blakeslee *et al.* (2003) found an intrinsic dispersion of 0.024 ± 0.008 mag for 30 ellipticals in the F775W - F850LP color, which approximates rest-frame $U - B$. This dispersion is comparable to that found by Bower *et al.* in Coma. Since some intrinsic color variation in the age and metallicity of stellar populations of the member galaxies is likely, the dispersion due to dust in these ellipticals must be smaller still, and we can confidently expect the observed smaller scatter of elliptical hosted SNe Ia at $z \sim 0.5$ to continue in $z \gtrsim 1$ cluster ellipticals. The precise *HST* color-magnitude diagrams now enabled by the proposed Cycle 15 data will *check* for dust in each cluster hosting a SNe, both for Cycle 14 and 15 SNe.

Why is this cluster search much more efficient at finding (and studying) SNe Ia at $z \gtrsim 1$ than the previous HST searches in the GOODS fields? By searching in rich clusters we find twice as many $z \gtrsim 1$ SNe in total as the previous blank-field searches (such as the two SN teams' previous GOODS searches), and *five times* as many SNe in elliptical hosts. The first 1/3 of the Cycle 14 search (75 orbits) already matches this rate (see Fig. 4b), with 4 new SNe in $z > 1$ ellipticals, and 1 new SN in a $z > 1$ cluster-member spiral (plus additional $z < 1$ SNe). Fig. 3a shows the reason for this dramatically enhanced discovery efficiency: compared to an average GOODS field our cluster fields generally contain 6 to 20 times the surface density of elliptical galaxies at $z \gtrsim 1$. Since we still find (and study) the field SNe not in clusters, the total discovery rate is more than double. (For comparison, the 2002-03 GOODS SNe search (Riess *et al.*2004) used 284 orbits to find and follow 3 $z > 1$ elliptical-hosted plus 4 spiral-hosted SNe.)

In addition to discovering more SNe Ia per HST orbit, there is another set of major efficiency gains in the *follow-up* of these SNe due to the knowledge of the host's elliptical morphology, the cluster redshift, and the higher rate per field. First, the follow-up observations need significantly less signal-to-noise and fewer bands, since the extinction correction no longer dominates the requirements. Second, the higher discovery rate allows pre-scheduling observations for each cluster with a cadence guaranteed to well sample the lightcurves for every SNe discovered. This completely *eliminates the need for rapid-turnaround ToO* follow-up! Finally, these $z \gtrsim 1$ clusters' old stellar populations (Glazebrook *et al.*2004, McCarthy *et al.*2004) will overwhelmingly host SNe Ia, so much spectroscopy can be saved as well.

Determination of Cluster Masses, and Dark Energy

The number of clusters of galaxies as a function of mass and redshift provides a powerful alternative probe of the cosmology thanks to its sensitivity to the comoving volume *and* the growth of large scale structure. The rare, massive clusters at high redshifts provide most of the discriminating power of the experiment, requiring large surveys of the sky to search for these systems. A number of large cluster surveys are underway (e.g., Red-sequence Cluster Survey and Blanco Cluster Survey) or imminent (e.g., South Pole Telescope Sunyaev-Zeldovich Survey, Dark Energy Survey) with this dark energy measurement as a key goal, but all require estimates for the cluster masses in order to successfully constrain cosmological parameters.

The observations proposed here will provide the most accurate calibration of the masses of high redshift clusters for years to come and will serve as the necessary reference to ensure that the next generation cluster surveys can reliably use clusters beyond $z \sim 1$ to constrain w to better than $5 - 10\%$. The recent work of Majumdar & Mohr (2003;2004) on "self-calibration" shows

that detailed study of only a moderate sample of clusters (such as that proposed here) can reach those goals. The combination of weak and strong lensing measurements, along with X-ray and SZ imaging of these clusters would provide much needed information for understanding the properties of the ICM at very high redshifts and therefore the role of clusters in cosmology.

Weak lensing measurements of cluster masses. Weak gravitational lensing of background galaxies is now a well-established technique for providing a *direct* measurement of the projected cluster mass, without any assumptions about the geometry or dynamical state of the cluster. The $z = 1 - 1.5$ range is of particular interest as it is the era where much of the cluster assembly is thought to occur. The sample studied here is 4 times larger than previous work, and targets clusters at higher redshifts. The additional Cycle 15 data will increase the effective number density of sources from ~ 100 to ~ 165 arcmin^{-2}, reducing the uncertainty in mass to 23% for the average cluster in our sample ($M = 5 \times 10^{14} M_{\odot}$). (These numbers are corroborated by preliminary weak lensing analysis of our Cycle 14 data.) Since the intrinisic scatter between mass measurements using various mass observables is $\sim$30% for the best-studied clusters (Yee & Ellingson 2003), our proposed Cycle 15 measurement would cross the threshold necessary to obtain robust information on the scatter of *individual* clusters about the mean relation.

The proposed observations enable us to determine the zero-point in the mass-observable relations to better than $10 - 15\%$ in each of four independent redshift bins. Furthermore, the improved accuracy in the mass measurements allows us to quantify the scatter (an often ignored, but critical part of cluster abundance studies) in these relations much better. These data will complement archival data and ground based efforts at lower redshifts (e.g., the Canadian Cluster Comparison Project, the CFHT Legacy Survey) that are undertaken by members of our team. Consequently, we will be able to study the evolution in the properties of clusters from the present day out to $z \sim 1.5$.

Strong lenses at $z \gtrsim 1$. Observations by ACS show image quality that dramatically increases the number of faint, low surface brightness strongly lensed arcs and image families detectable – particularly with the new use of multicolor data we propose for Cycle 15. Our cluster sample already contains 3 new giant arc systems lensed by $z \gtrsim 1$ clusters, doubling the number known, including a giant arc behind the highest redshift lensing cluster to date. A single arc in a high redshift cluster determines the mass interior to the Einstein radius (~ 100 kpc/h), and when combined with our complementary larger scale weak lensing analysis will measure the concentration parameter of the dark matter halo. In addition, comparison with results at lower redshifts enables us to follow the evolution of strong lensing cluster abundances and characteristics, and test CDM predictions (Hennawi *et al.* 2006). Our unprecendented deep imaging survey of high redshift clusters will allow us to place the first constraints on the profiles of dark matter halos at $z \gtrsim 1$.

X-ray and SZ cluster synergy. We have been successful in getting XMM and Chandra time for the cluster observations and have agreements with the PI of SPT and SZ Array, John Carlstrom, to obtain Sunyaev-Zeldovich measurements. This multiwavelength strategy of determining cluster masses through lensing, X-ray, and SZ enables significant advances in understanding cluster physics and formation.

Galaxy Cluster Science at $z \gtrsim 1$

Whether they form via monolithic collapse (Eggen, Lynden-Bell & Sandage 1962) or hierarchical assembly (White & Frenk 1991), massive elliptical galaxies account for a substantial

fraction of the stellar mass in the Universe (Hogg *et al.* 2002), and are found in highly overdense regions (Dressler 1980; Hogg *et al.* 2003) - i.e., galaxy clusters. The slope, scatter, and intercept of the cluster elliptical galaxy color magnitude relation at $z < 1$ are surprisingly well matched by a simple star formation history consisting of a burst at $z > 3$ followed by passive evolution (Stanford *et al.* 1998), and their luminosity functions also are fit by such models (de Propris *et al.* 1999). ACS imaging of more distant clusters will determine how far this scenario can be pushed, by enabling measurements of the merger and elliptical fractions, their luminosity functions – and new in this proposal – precise measurements of the color-magnitude relation (CMR).

Postman *et al.* (2005) use morphological analyses of ACS GTO imaging of 7 $0.8 < z < 1.3$ clusters to show that the fraction of ellipticals does not change up to $z \sim 1.25$, and that the fraction of S0s remains roughly constant at the 20% level seen in $0.4 < z < 0.5$ clusters. Hence, the formation of all massive cluster ellipticals, and a significant fraction of the lenticulars as well, must be occurring at $z > 1.25$. This is supported by limits on the most recent star formation from the small dispersion and lack of evolution of the CMR's out to $z \sim$1 (see Figure 3).

This proposal takes the next step beyond the existing small sample and upper redshift to probe the regime in which massive cluster galaxies are being formed. The GTO program has three clusters at $z > 1$, while our sample has 20. The highest redshift of the clusters is pushed from $z = 1.27$ to $z = 1.5$. Moreover, the addition of Cycle 15 images will vastly improve measurements of the mean and dispersion of the CMR, limiting the time of the most recent epoch of star formation. In conjunction with data we have obtained from Chandra, XMM, Keck, Subaru, the VLT, Magellan, and Spitzer, the ACS data to be obtained in this proposal will determine the epochs of the assembly of ellipticals and the origin of S0s, and calibrate the relation between mass and X-ray luminosity and temperature (and future SZ mass determinations) at these redshifts.

Supernovae rates and star formation The rate of SNe in galaxy clusters will address outstanding questions about the ICM, in particular its high metallicity and energetics. The iron that would be produced by a Salpeter IMF by Type II SNe is insufficient to explain the [Fe/H] in the ICM; furthermore, type Ia's at their current rate are also insufficient. However, if SNe Ia's exploded at a higher rate in the past (Bighenti & Mathews 1999), they could be significant contributors to the excess entropy seen in the ICM (e.g., Pipino *et al.* 2002) Gal-Yam *et al.* (2002) estimates rate of $0.41^{+1.23}_{-0.39} h^2_{50}$ SNu from HST archival images of $z < 1$ SNe in 9 clusters. This suggests that SNe Ia may not be the dominant source of iron in the ICM, but the ~ 20 SNe Ia in $z > 1$ clusters expected from our program will allow a first statistically meaningful test of this idea. The ICM may hide a significant number of stars stripped from galaxies in an unobservable low-surface-brightness population bound to the cluster halo. This would bias cluster mass measurements and other cluster mass observables inferred from the (passively evolving early-type) stellar component of cluster galaxies (e.g. Yee & Ellingson 2003, Lin, Mohr & Stanford, 2004) in several large upcoming surveys (e.g. RCS-2, DES). Our Cycle 15 statistics will for the first time be able to directly constrain the fraction of 'hostless' SNe and hence provide a direct estimate (at the 5-10% level) of the fraction of stars in the ICM at high redshift, for comparison with deep ground-based observations of local clusters (e.g. Ting & Mohr 2004; Mihos *et al.*2005)

Conclusions

The observations proposed capitalize on our new approach to high-redshift SNe measure-

ments and will provide a first significant, *and unbiased* measurement of w_0 vs. w'. They will then comprise a springboard for a wide array of astrophysical investigations: high redshift SNe, cluster profiles, gravitational lensing, and multiwavelength studies of large scale structure and cosmology. The emphasis on high redshift and attention to systematics is essential for bringing to maturity key next-generation cosmological techniques, while the cluster data will serve as a bedrock scientific legacy for extragalactic astronomy.

References

⊙ Blakeslee, J. *et al.*2003, ApJL, 596, 143 ⊙ Bower, R. *et al.*1992, MNRAS, 254, 589 ⊙ Broadhurst, T. *et al.*2005, ApJ, 621, 53 ⊙ Brodwin, M. 2006, ApJ, subm. ⊙ De Propris, R. *et al.*1999, AJ, 118, 719 ⊙ Donahue, M. & Voit, G. M. 1999, ApJ, 523, 137 ⊙ Draine, B. 2003, ARA&A 41, 241 ⊙ Dressler, A. 1980, ApJ, 236, 351 ⊙ Eggen, O. *et al.*1962, ApJ, 136, 748 ⊙ Eke, V. *et al.*1998, ApJ, 503, 569 ⊙ Ellis, R. *et al.*1997, ApJ, 483, 582 ⊙ Elston, R. *et al.*2006, ApJ in press ⊙ Fadeyev, V. *et al.*2004, AAS, 205, 69.03 ⊙ Glazebrook, K. *et al.*2004, Nature, 430, 181. ⊙ Gal-Yam, A. *et al.*2002, MNRAS, 332, 37 ⊙ Gioia, I. *et al.*1990, ApJ, 356, L35 ⊙ Hennawi, J. 2006, ApJ, subm. ⊙ Henry, J. 2000, ApJ, 534, 565 ⊙ Henry, J. & Arnaud, K. 1991, ApJ, 372, 410 ⊙ Hogg, D. *et al.*2002, AJ, 124, 646 ⊙ Hogg, D. *et al.*2003, ApJ, 585, 5 ⊙ Hogg, D. *et al.*2004, ApJ, 601, 29 ⊙ Holden, B. *et al.*2004, AJ, 128, 3034 ⊙ Jee, M. *et al.* 2005, ApJ, 618, 46 ⊙ Jee, M. *et al.* 2006, ApJ, in press ⊙ Knop, R. *et al.* 2003, ApJ, 598, 102 ⊙ Lidman,C. *et al.*2004, A&A, 416, 829 ⊙ Lin, Y-T., Mohr, J.J., & Stanford S.A. 2004, ApJ, 610, 745. ⊙ Lombardi, M. *et al.*2005, ApJ, in press ⊙ Majumdar, S. & Mohr, J. 2003, ApJ, 586, 603 ⊙ Majumdar, S. & Mohr, J. 2004, ApJ, 613, 41 ⊙ Mihos, J. *et al.*2005, ApJ, 631, 41 ⊙ McCarthy, P. *et al.* 2004, ApJ, 614, L9 ⊙ Nichol, R. *et al.*1999, ApJ, 521, L21 ⊙ Pain, R. *et al.*1997, ApJ ⊙ Pasquali, A *et al.*2006), ApJ, 636, 115 ⊙ Perlmutter, S. *et al.*1999, ApJ, 517, 565 ⊙ Pipino, A. *et al.*2002, NewA, 7, 227 ⊙ Postman, M. *et al.*2005, ApJ, 623, 721 ⊙ Riess, A. *et al.*2004, ApJ, 607, 665 ⊙ Rosati, P. *et al.*1998, ApJ, 492, L21 ⊙ Rosati, P. *et al.*1999, AJ, 118, 76 ⊙ Rosati, P. *et al.*2001, ⊙ Rosati, P. *et al.*2004, AJ, 127, 230 ⊙ Stanford, S. *et al.*1997, AJ, 114, 2232 ⊙ Stanford, S. *et al.*2001, ApJ, 552, 504 ⊙ Stanford, S. *et al.*2002, AJ, 123, 619 ⊙ Stanford, S. *et al.*2002, AJ, 123, 619 ⊙ Stanford, S. *et al.*2004 ⊙ Sullivan, M. *et al.*2003, MNRAS, 340, 1057 ⊙ Temi, P. *et al.*2005, ApJ, 635, L25 ⊙ Ting, Y-T. & Mohr, J. 2004, ApJ, 617, 879 ⊙ Tran, H. D. *et al.*2001, AJ, 121, 2928 ⊙ van Dokkum, P. *et al.*2001, ApJ, 552, 101 ⊙ Vikhlinin, A. *et al.* 1998, ApJ, 498, L21 ⊙ White, S. & Frenk, C. 1991, ApJ, 379, 52 ⊙ Yee, H. & Ellingson, E. 2003, ApJ, 585, 215

Description of the Observations

The supernova observing strategy

The high rate of SNe Ia produced in clusters *in addition* to the SNe Ia in the fore/background field galaxies makes possible an elegantly simple combined search-and-follow-up scheduling strategy, which we are now successfully demonstrating in cycle 14. We observe each cluster for one orbit every $\sim$21-24 days for $\sim$8 visits, where the exact cadence depends on the cluster redshift and the exact number of visits depends on HST observing constraints. Every SN that appears in these clusters and fields, modulo small end effects, has a fully sampled lightcurve in two bands (each orbit contains four ACS/F850LP dithered cosmic-ray splits plus one, longer ACS/F775W exposure)— without the need for expensive Target of Opportunity (ToO) observations (see Fig. 5a). We obtain ground-based spectroscopy for precise redshifts and confirmation of elliptical galaxy type (which confirms SN Ia identification), and/or a spectrum of the SN itself (Fig. 5b). We always discover the SN early enough (Fig. 5a) that we can use a ($>$2-week-advance-notice) low impact ToO for additional NIC2 F110W observations within $\pm$5 days of the SN lightcurve peak for all SNe above $z > 1$. Only for the highest redshift SNe Ia $z > 1.4$ is a full 11-orbit lightcurve with NIC2 F110W taken. (NICMOS fields are too small to be used in the search.)

We use the F775W-F850LP color to correct field-galaxy SNe for extinction, and both F850LP-

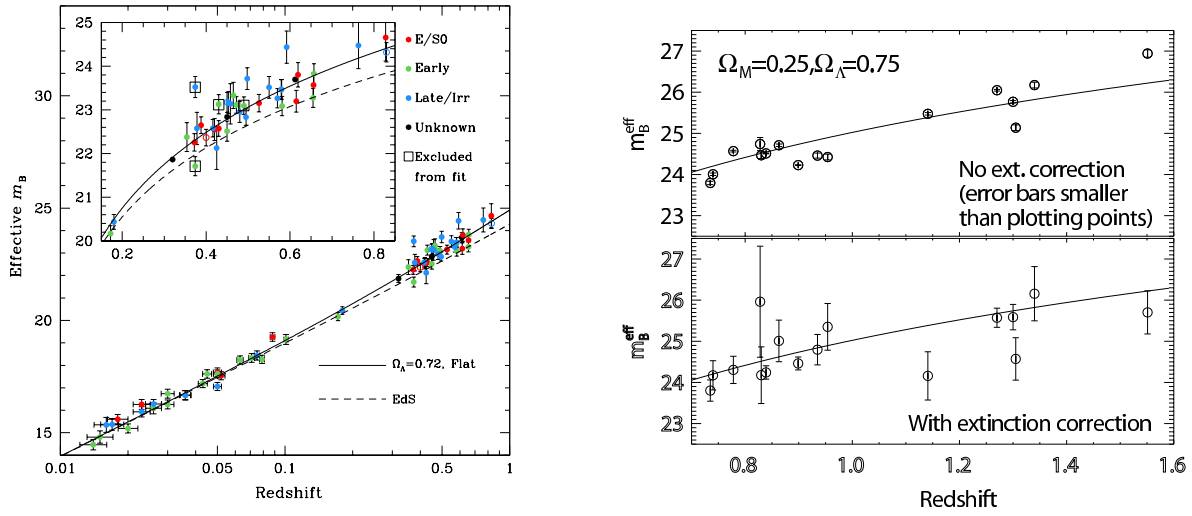

Figure 1: **(a) Left Panel:** The SCP SNe Ia Hubble diagram broken into host galaxy types from Sullivan et al. (2003). The SNe in elliptical hosts (filled red circles) show significantly less dispersion, $\sigma = 0.16$ mag, including measurement error. (This ground-based measurement error for this $z \sim 0.5$ sample is quite close to the HST measurement error at $z > 1$ in this proposal.) **(b) Right Panel:** The comparison of the Hubble diagram, before and after extinction correction, for a mixture of SNe Ia in all host types shows the dramatic increase in error bars due to the uncertainty in $B - V$ color being multiplied by $R_B \approx 4$ and by the uncertainty in R_B. The data shown is from the SCP (Knop et al. 2003) and the Riess et al. 2004 GOODS search samples. For the SNe at redshifts $z > 1$ this yields an uncertainty of ∼0.5 mag, which is consistent with the measured dispersion of 0.5 mag. The ratio of this dispersion to the elliptical-hosted dispersion of panel (a) makes the elliptical-hosted SNe each worth 6 to 9 of the extinction-corrected others.

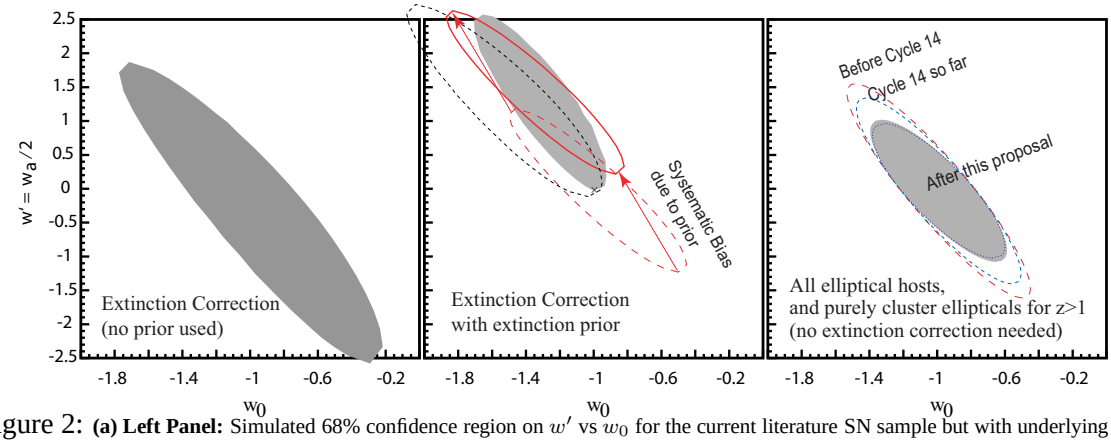

Figure 2: **(a) Left Panel:** Simulated 68% confidence region on w' vs w_0 for the current literature SN sample but with underlying cosmology ($w_0 = -1$; $w' = 0$). The parameters are poorly constrained because color errors are magnified by $R_B \approx 4$. **(b) Middle Panel:** The solid red contour shows reduced uncertainties (excluding systematic bias) using a Baysian prior on the extinction distribution prior to suppress color errors. The short-dashed contour shows that this approach is sensitive to precise knowledge of R_B and its variation with redshift; the example shifts from 4.1 to 2.6. Similarly, asymmetric priors can also introduce systematic biases (arrows). The filled gray contour is from Riess *et al.* 2004 using such a prior. **(c) Right Panel:** Simulated 68% region for the proposed new set of ~ 20 $z \gtrsim 1$ SNe Ia found in cluster ellipticals (from Cycle 14 & 15) if combined with 120 SNe Ia in ellipticals at the lower redshifts now being produced by the ground-based CFHT SNe Legacy Survey, the CTIO Essence survey, and (at $z < 0.1$) the Nearby SNe Factory. This approach addresses the large statistical error problem of panel (a) and the systematics problem of panel (b). The projected constraints from the ground-based surveys alone are given by the the outer contour, and the constraints from adding the 3 cluster-elliptical SNe found so far in the first third of Cycle 14 are the dashed contours. The almost-imperceptably-smaller innermost (dotted) contour shows the effect of adding ~ 10 SNe in *field* ellipticals (if one is willing to risk using them at $z > 1$ along with the *cluster* ellipticals), also expected from Cycle 14 and 15 as well as from previous GOODS surveys.

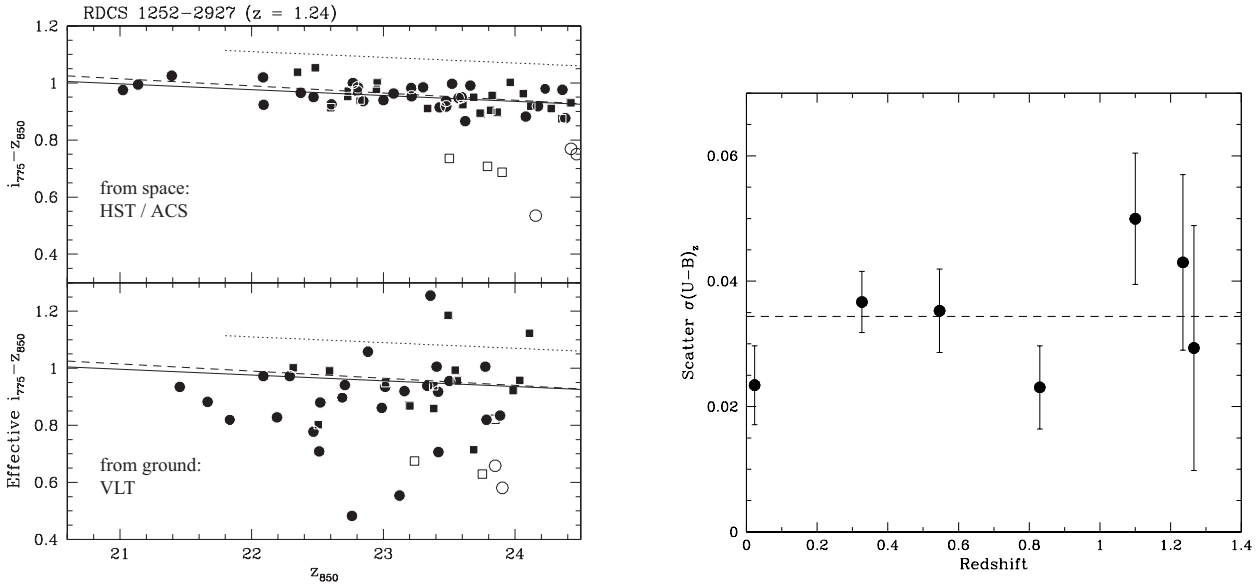

Figure 3: **(a) Left Panel:** The dust-free nature of cluster ellipticals (circles) and S0 galaxies (squares) in RDCS 1252-2927 at $z = 1.24$ is supported by the small scatter of the color-magnitude relation (CMR) when ACS quality photometry is used (from Blakeslee *et al.* 2003). The CMR in this same cluster using data from the VLT FORS and ISAAC (transformed to the ACS i,z passbands) exhibits nearly 8 times the scatter demonstrating the need for HST imaging. With this large ground-based scatter, the outliers from the space-based CMR (indicated by open symbols) cannot be distinguished. **(b) Right Panel:** The scatter about the early-type red sequence in clusters from $0.02 < z < 1.3$. The three clusters at $z > 1$ are RDCS0910+5422, RDCS1252-2927, and RDCS0848+4452 – in both the GTO cluster survey and this SNe survey.

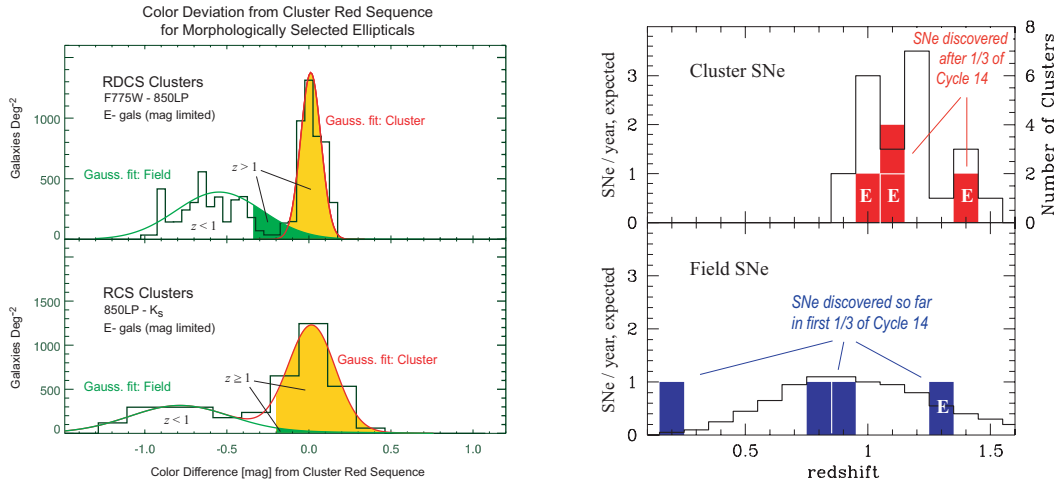

Figure 4: **(a) Left Panel:** The overdensity of $z > 1$ ellipticals achieved by centering on $z > 1$ clusters is typically in the range 6 - 20. The histograms show the color distribution of field ellipticals (nearly all at $z < 1$) and red sequence cluster ellipticals relative to the mean color of the red sequence galaxies. Also shown are the best fit Gaussians to the field and red sequence elliptical galaxy color distributions, where the gaussian fit to the field is based on additional ACS fields with no clusters. Galaxies with colors indicating $z > 1$ are shown by the filled regions under the gaussian fits. The top panel is a composite from 3 clusters from the GTO at redshifts of $z = 1.10,\ 1.24$ and 1.27. The bottom panel shows the same for two RCS clusters at $z = 0.95$ and 1.03. **(b): Right Side:** The upper panel shows the redshift distribution of the expected number of SNe per year in the clusters (left axis) and the number of clusters being searched (right axis). The actual cluster SNe that have been found so far in our Cycle 14 data are indicated by filled boxes (E indicates an elliptical host.) The lower panel shows the redshift distribution of the expected number of SNe per year in the field, with the actual field SNe discovered so far indicated by filled boxes.

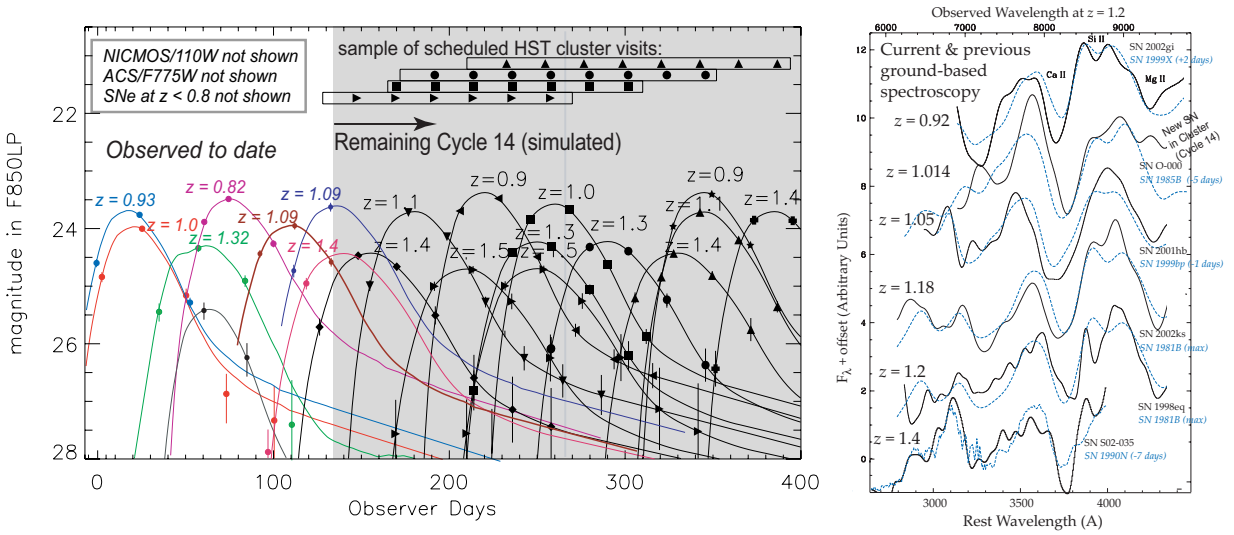

Figure 5: **(a) Left Panel:** The unshaded region to the left displays the preliminary lightcurves of the 8 SNe discovered in the first third of Cycle 14, while the shaded region shows simulated data for the remaining two-thirds. With our chosen cadence, which is also proposed for cycle 15, we obtain typical fit peak magnitude total uncertainties of 0.07 to 0.15 mag, including the lightcurve time stretch correction uncertainty. **(b): Right Panel:** Ground-based spectra (VLT, Keck, Subaru) in the redshift range 0.9 – 1.4 (solid curves) de-redshifted to the SN restframe. Host galaxy light has been removed and a low-pass filter applied to remove any unrelated features, i.e. with widths narrower than that of a SN. The spectrum second from the top is that of the first cluster SN discovered in our cycle 14 program. The other spectra were obtained in previous SCP SN campaigns and are shown to demonstrate ground-based spectroscopy out to z=1.4. For each spectrum, a matching template spectrum from a well-studied nearby SN is shown (dashed curves).

F110W and F775W-F850LP colors to study intrinsic colors – and its possible relation to luminosity – for SNe in cluster and field elliptical hosts (which will greatly help the calibration of the GOODS SNe). For $z \lesssim 1.25$, these are B-V and U-B restframe colors, and for $z \gtrsim 1.25$ these are U-B and a UV color (less useful, but free). The CFHT SN Legacy Survey (of which 3 members are co-I's on this proposal) has used well observed SNe at $z \approx 0.3$ to show that restframe U-B color is an excellent calibrator of SN Ia corrections for dust or other intrinisc-color dependencies, to a precision below the intrinsic SN Ia dispersion. The fluxes/magnitudes, cadence and error bars shown in Fig. 5a demonstrate the signal to noise obtained with our cadence and exposure times. For the bulk of the target clusters up to z=1.3 these lightcurves will yield a distance modulus uncertainty below the ∼0.15 mag intrinsic SNe Ia uncertainty (in fact, 90% of the SNe will have uncertainties below 0.10 mag).

In summary we require 185 pre-scheduled search orbits, as well as 32 ToO orbits for the observation of 12 SNe using NIC2 F110W (8 single-orbit ToOs for SNe with $1 \lesssim z \lesssim 1.25$; two 2-orbit observations for SNe with $1.25 \lesssim z \lesssim 1.4$ and two 11-orbit sequence ToO scheduled over approximately 6 weeks needed to obtain the restframe B lightcurve for the SNe at $z \gtrsim 1.4$).

Utilizing deep references images: Deep ACS reference images are available from cycle 14 to determine the fraction of flux from the host galaxy in the observed lightcurves. The gain in SNR is $\gtrsim$25%, making it possible to find SNe earlier and determine the lightcurve parameters with higher precision. This gain in SNR will also make possible a longer F775W exposure time of 515 seconds per orbit, while the four F850LP exposures needed for searching are reduced to 340 seconds each

(the optimal ratio for a color measurement of both SNe and cluster galaxies).

For $\sim$2 of the targeted SNe observed with NICMOS we expect the SNe to be so close to the core of a bright host that we will need an additional final image after the SNe has faded, with a 3-orbit depth so as not to degrade the signal-to-noise after subtraction. Offsetting this requirement for 6 additional orbits is the probability of canceling the final two cadence observations for clusters that have not produced a SNe in time to be followed for sufficient lightcurve points. This happens often enough (and 3 weeks in advance) that we can reschedule these canceled final observations to provide the post-SNe visit for the cases that require them without major scheduling complications.

Spectroscopic identification and redshift determination: Our team has large associated ground-based programs at Subaru (10 half-nights per semester), VLT (16 hours queue time), Keck (2 nights per semester), and Magellan (10.5 nights per semester), providing host galaxy and/or SNe spectra for every one of the $>$20 SNe. (Fig. 5a shows that some of our SNe are always observable.) The host spectra confirm redshift and elliptical identity for every host – thus confirming Type Ia status for those without a "live" spectrum. Note that this host galaxy data is sufficient to give $>$90% confidence that we have identified a Type Ia; this is comparable to the success rate with spectroscopic ID's at these redshifts (from ground or HST). Fig. 5b shows that ground-based spectra for SNe Ia at redshifts as high as $z \sim 1.4$ are able to identify the SNe comparably to ACS/grism. (Fig. 5b includes one SN spectrum from a cycle 14 SN. Three additional SN spectra are scheduled for observation in the coming week. Not shown are host galaxy spectra for all the cycle 14 SNe.) At still higher redshifts the ACS/grism can occasionally obtain a usable spectrum, but at a cost of over 12 orbits. This is unnecessary for SNe in a well-confirmed cluster elliptical host, and for a possibly dusty spiral we would rather use the same number of orbits to find a new –much more useful – elliptical-hosted SN!

Observing requirements for the cluster science

The observational requirements for the cluster science are driven by the goals associated with characterizing the formation and evolution of the cluster galaxies. These requirements include **(1)** obtaining reliable morphological classifications (performed both visually and via machine algorithms) to 2 magnitudes below L^* at $z \sim 1.2$ (~ 24 AB mag in 850LP) using the standard system of elliptical, lenticular, and spiral/irregular over an area reaching out to r_{200}, **(2)** measurement of the slope and intercept of, and intrinsic scatter about, the early-type red sequence to a precision of $\lesssim 20\%$ and **(3)** deriving galaxy effective radii with sufficient accuracy to enable estimates of M/L ratios for early-type galaxies when coupled with velocity dispersions from on-going ground-based programs. Goal (1) requires an integrated S/N $\gtrsim$ 25 over the central 10 kpc of the galaxy; Goal (2) requires colors with uncertainties $\lesssim 0.10$ mag at the above classification limit (24 AB mag) – this requirement is driven by the small scatter ($\sim$0.025 mag) already observed at these redshifts and Goal (3) is well satisfied by the constraint imposed by the first two. From data already in hand we determine that the S/N of photometry for galaxies with AB mag ≤ 24 will meet or beat all these requirements with a total exposure of $\sim 3,800$ seconds and $\sim 10,000$ seconds in F775W and F850LP, respectively. The list of targeted clusters is based on those observed in Cycle 14. With high redshift cluster searches currently ongoing (RCS-2, XMM, IRAC) we might substitute a new-found, even richer cluster before Phase 2.

Observing requirements for the weak lensing studies

To compute the accuracy with which we can determine the masses of clusters we used data from the UDF to determine the "effective" number density of sources used in the lensing analysis. These estimates include a proper weighting for the smaller sources which have sizes comparable to the PSF. We find excellent agreement when these numbers are compared to the results obtained with clusters already observed. The proposed exposure times (75% F850LP and 25% F775W) give similar source densities in both filters and, combining measurements in both filters, yields the estimated accuracy in mass determination given above in the Scientific Justification. These calculations also agree well with published results (Jee et al. 2005,2006; Lombardi et al. 2005).

Many other HST weak lensing cluster studies have used a mosaic to measure the lensing signal out to large radii, in an effort to break the mass-sheet degeneracy. Our detailed calculations show that the gain from mosaicing is minimal for clusters beyond $z = 1$ (where the FOV of ACS is well matched to the angular extent of the cluster), and that it is instead deeper observations that provide more accurate masses.

Ground-based observations

Extensive ground-based observations of the target clusters have been carried out and will continue to be performed at Keck, Magellan, and the VLT. Deep multiband imaging exists for all target clusters, including in most cases optical and NIR bands. An abundant amount of multiwavelength data has already been published for the three X-ray clusters (Stanford et al. 1997, Rosati et al. 1999, Stanford et al. 2001, Stanford et al. 2002, Rosati et al. 2004, Lidman et al. 2004, Holden et al. 2004). In particular, we have spectroscopic redshifts for the brightest $\sim$ 20 member galaxies on average for each of these RDCS clusters so the redshifts of the likely host galaxies for SNe to be found in this HST program are already known. For the IRAC clusters, we have begun a program of slitmask spectroscopy at Keck (Stanford et al 2005, Elston et al 2006, Brodwin et al 2006) to obtain redshifts for the brightest galaxies which should provide spectroscopic-z for galaxies containing $\sim$50% of the total cluster luminosity within the next $\sim$2 years.

Special Requirements

As described in the Observing Strategy, we only require $>$2-week-advance-notice ToO's (for 12 targets). In association with these NICMOS ToOs we request 34 orbits of Coordinated Parallel ACS observations. Because clusters accrete much of their mass at late times, many galaxies residing in clusters at $z = 0$ lie outside the central 900 kpc (ACS FOV) at $z > 1$. ACS+NICMOS parallels afford an extended view of cluster formation. The NICMOS-ACS offset corresponds to 2.2 Mpc at $z = 1.4$ – comparable to the virial radius at $z = 0$.

Coordinated Observations

Justify Duplications

Every proposed observation will search for, or follow-up, new SNe. Previous ACS observations of these targets will provide deeper reference images, important help for the SN search.